

Improved nuclear model with derivative scalar couplings and ρ -meson mass at finite temperature and density

Ping Wang,¹ Zhiwei Chong,¹ Ru-Keng Su,^{2,1} and P. K. N. Yu³

¹Department of Physics, Fudan University, Shanghai 200433, People's Republic of China

²Chinese Center of Advanced Science and Technology (World Laboratory), P.O. Box 8730, Beijing 100080, People's Republic of China

³Department of Physics and Materials Science, City University of Hong Kong, Tat Chee Avenue, Kowloon, Hong Kong, People's Republic of China

(Received 17 August 1998)

An improved nuclear model with derivative scalar couplings is proposed. It includes the freedoms of nucleons, σ mesons, ω mesons, and ρ mesons. Employing the thermofield dynamics, we have calculated the self-energy Feynman diagrams of ρ meson and found the temperature and density dependence of the ρ meson. We found that the density dependence of the ρ meson given by this model is in good agreement with recent experimental results. [S0556-2813(99)03002-2]

PACS number(s): 14.40.Cs, 24.10.Jv, 13.75.Cs

I. INTRODUCTION

The Zimanyi-Moszkowski (ZM) model [1] is one of the useful models in explaining many experimental properties of both nuclear matter and finite nuclei in mean field approximation (MFA) [2–5]. This is a nuclear model with derivative scalar couplings. It has a softer equation of state and a reasonable compression modulus $K=225$ MeV when compared to those of the Walecka model [6]. In our previous works [7–9], by using the real time Green's function method and the pair-cutoff approximation [10], we extended the ZM model to finite temperature and density. We investigated the liquid-gas phase transition of nuclear matter and the fluctuations of the meson field of this model and found that the ZM model is suitable in describing many physical properties of nuclear systems even at finite temperature and density. A recent paper by Malheiro *et al.* [2] confirmed this conclusion.

However, as pointed out by Refs. [8,11,12], there are two main shortcomings in the ZM model. One refers to the spin-orbit splitting [12]. The effective mass M^* of nucleon at saturation density given by the ZM model in MFA is $M^*/M=0.85$. It is too large and will almost certainly have small spin-orbit splitting for finite nuclei because the mean fields are small. To overcome this difficulty, Biro and Zimanyi [13] added a tensor coupling term of $NN\omega$ interaction to the ZM Lagrangian and proved that the description of the spin-orbit term is justified without changing other MFA results of the ZM model. In Ref. [11], we studied the effect of tensor coupling term on the properties of an unpolarized hot medium and proved that the vacuum fluctuation effect of tensor interaction in the ZM model on the liquid-gas phase transition is very small. Therefore, the addition of a tensor coupling term to the ZM Lagrangian is successful because it not only improves the spin-orbit splitting in finite nuclei, but also does not change the thermodynamical properties of nuclear matter. The second shortcoming of the ZM model refers to isospin independence [8,9]. In Ref. [9], we pointed out that when we employed the ZM model to investigate

asymmetric nuclear matter, a lot of difficulties, e.g., Coulomb instability and negative asymmetric parameter in the vapor phase, will emerge because this model is isospin independent. To overcome these difficulties, we added a ρ -meson freedom into the ZM model [9].

According to the above arguments, instead of the rescaling ZM Lagrangian [1]

$$L_{ZM} = -\bar{\psi}M^*\psi + \bar{\psi}i\gamma^\mu\partial_\mu\psi - g_\omega\bar{\psi}\gamma_\mu\omega^\mu\psi + \frac{1}{2}(\partial_\mu\sigma\partial^\mu\sigma - m_\sigma^2\sigma^2) - \frac{1}{2}F_{\mu\nu}F^{\mu\nu} + \frac{1}{2}m_\omega^2\omega_\mu\omega^\mu, \quad (1)$$

where M^* is the effective mass of nucleon,

$$M^* = fM, \quad f = \left[1 + \frac{g_\sigma\sigma}{M}\right]^{-1}. \quad (2)$$

We suggested an improved ZM Lagrangian without the above two shortcomings as

$$L_{IZM} = -\bar{\psi}M^*\psi + \bar{\psi}i\gamma^\mu\partial_\mu\psi - g_\omega\bar{\psi}\gamma_\mu\omega^\mu\psi + \frac{f_\omega}{4M^*}\bar{\psi}\sigma^{\mu\nu}(\partial_\mu\omega_\nu - \partial_\nu\omega_\mu)\psi - g_\rho\bar{\psi}\gamma_\mu\vec{\tau}\cdot\vec{b}^\mu\psi - \frac{f_\rho}{4M^*}\bar{\psi}\sigma^{\mu\nu}\vec{\tau}\cdot(\partial_\mu\vec{b}_\nu - \partial_\nu\vec{b}_\mu)\psi - \frac{1}{4}F_{\mu\nu}F^{\mu\nu} + \frac{1}{2}m_\omega^2\omega_\mu\omega^\mu - \frac{1}{4}\vec{B}_{\mu\nu}\cdot\vec{B}^{\mu\nu} + \frac{1}{2}m_\rho^2\vec{b}_\mu\cdot\vec{b}^\mu + \frac{1}{2}(\partial_\mu\sigma\partial^\mu\sigma - m_\sigma^2\sigma^2), \quad (3)$$

where

$$F_{\mu\nu} = \partial_\mu\omega_\nu - \partial_\nu\omega_\mu, \quad \vec{B}_{\mu\nu} = \partial_\mu\vec{b}_\nu - \partial_\nu\vec{b}_\mu,$$

$$\sigma_{\mu\nu} = \frac{i}{2} [\gamma_\mu, \gamma_\nu] \quad (4)$$

and $\vec{\tau}$ is the isospin operator. In Eq. (3), σ , ω_μ , and \vec{b}_μ are the neutral scalar meson field, the ω -meson field, and the ρ -meson field with the corresponding masses m_σ , m_ω , and m_ρ , and the corresponding coupling constants g_σ , g_ω , g_ρ , f_ω , and f_ρ , respectively. The basic extensions of L_{IZM} are not only the tensor coupling terms of the $NN\omega$ interaction, but also the isospin-dependent ρ -meson field.

On the other hand, the deduction of the ρ -meson field in a hot and dense medium has attracted much attention recently. Experiments from HELIOS-3, CERES, and NA50 Collaborations at SPS/CERN energies have shown that there exists a larger excess of lepton pairs in central S+Au, S+W, Pb+Au, and Pb+Pb collisions [14]. These experimental results may give a hint of some changes of hadron properties in nuclei. To explain the dilepton enhancement in hadronic matter, many workers used different approaches including transport studies [15], a dispersion relation for scattering amplitude at low density [16,17], spectral distributions of current correlation functions in baryonic matter [18,19], and changes of the ρ propagator in the $\rho\pi\pi$ interaction or vector dominance model [20,21] to investigate the dropping of ρ meson mass. Furthermore, a recent experiment of the TAGX Collaboration [22] has shown that when the density of the medium equals to $0.7\rho_0$ where ρ_0 is the saturation density, the mass of the neutral ρ meson reduces to 610 MeV. Many theoretical treatments including Brown-Rho scaling [23],

QCD sum rules [24], the quark-meson coupling model [25], vacuum polarization Feynman diagram calculations [26–28], etc., have been employed to explain the experimental results. Unfortunately, however, the mass reduction of the ρ meson observed is significantly different from the theoretical predictions mentioned above [23–28]. It is therefore of interest to explore another model to study this problem.

This paper evolves from an attempt to investigate the density dependence of the ρ -meson mass by using the improved ZM model. The thermofield dynamics (TFD) is used to sum the $NN\rho$ self-energy Feynman diagrams and calculate the effective mass and the screening mass of the ρ meson. The coupling constant g_ρ of the $NN\rho$ interaction is chosen to fit the symmetry energy 33.2 MeV of the nuclear matter. Another coupling constant f_ρ is given by the strong coupling and weak coupling approaches, respectively. We will prove that the reduction of ρ -meson mass given by this model is in good agreement with present experiments of the TAGX Collaboration [22].

In the next section, the formalism is given. The results and discussions will be presented in the last section.

II. FORMALISM

A. Equations of motion and mean fields of mesons

The equations of motion for nucleon and σ -, ω -, and ρ -meson fields can be easily derived from the improved Lagrangian L_{IZM} :

$$\begin{aligned} & \left[\gamma^\mu (i\partial_\mu - g_\omega \omega_\mu - g_\rho \vec{\tau} \cdot \vec{b}_\mu) + \frac{f_\omega}{4M^*} \sigma^{\mu\nu} F_{\mu\nu} - \frac{f_\rho}{4M^*} \sigma^{\mu\nu} \vec{\tau} \cdot \vec{B}_{\mu\nu} - M^* \right] \psi = 0, \\ & -\partial_\mu \partial^\mu \sigma - m_\sigma^2 \sigma + \frac{M^*}{M^2} g_\sigma \bar{\psi} \psi + \frac{g_\sigma f_\omega}{4M^2} \bar{\psi} \sigma^{\mu\nu} F_{\mu\nu} \psi - \frac{g_\sigma f_\rho}{4M^2} \bar{\psi} \sigma^{\mu\nu} \vec{\tau} \cdot \vec{B}_{\mu\nu} \psi = 0, \\ & \partial_\mu \left(F^{\mu\nu} + \frac{f_\omega}{2M^*} \bar{\psi} \sigma^{\mu\nu} \psi \right) + m_\omega^2 \omega^\nu - g_\omega \bar{\psi} \gamma^\nu \psi = 0, \\ & \partial_\mu \left(\vec{B}^{\mu\nu} - \frac{f_\rho}{2M^*} \bar{\psi} \sigma^{\mu\nu} \vec{\tau} \psi \right) + m_\rho^2 \vec{b}^\nu - g_\rho \bar{\psi} \gamma^\nu \vec{\tau} \psi = 0. \end{aligned} \quad (5)$$

For an unpolarized medium, $\langle \bar{\psi} \sigma_{\mu\nu} \psi \rangle = 0$. The mean fields of the mesons satisfy

$$\sigma = \frac{1}{m_\sigma^2} \frac{M^{*2}}{M^2} g_\sigma \langle \bar{\psi} \psi \rangle, \quad (6)$$

$$\omega_0 = \frac{g_\omega}{m_\omega^2} \langle \psi^+ \psi \rangle = \frac{g_\omega}{m_\omega^2} (\rho_p + \rho_n), \quad (7)$$

$$\rho_0 = \frac{g_\rho}{m_\rho^2} \langle \psi^+ \tau^0 \psi \rangle = \frac{g_\rho}{m_\rho^2} (\rho_p - \rho_n). \quad (8)$$

The internal energy per nucleon (E/B) in nuclear matter at a given temperature and a given density $\rho = \rho_p + \rho_n$ can be expressed as

$$\begin{aligned} E/B = & \frac{2}{\rho(2\pi)^3} \int d^3k E^*(k) [n_n(k) + \bar{n}_n(k) + n_p(k) + \bar{n}_p(k)] \\ & + \frac{m_\sigma^2}{2\rho} \sigma^2 + \frac{g_\omega^2}{2m_\omega^2} \rho + \frac{g_\rho^2}{2m_\rho^2} (\rho_p - \rho_n)^2, \end{aligned} \quad (9)$$

where

$$E^*(k) = \sqrt{k^2 + M^{*2}}. \quad (10)$$

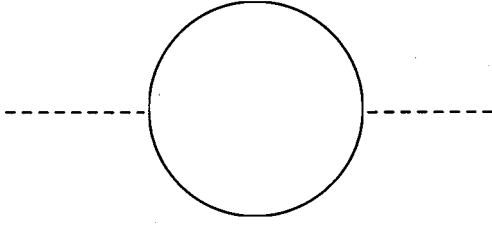


FIG. 1. The self-energy Feynman diagram of the ρ meson.

$n_F(k)$ and $\bar{n}_F(k)$ ($F=n,p$) are the nucleon and antinucleon distributions

$$n_F(k) = \frac{1}{e^{\beta(E^* - \nu_F)} + 1},$$

$$\bar{n}_F(k) = \frac{1}{e^{\beta(E^* + \nu_F)} + 1} \quad (F=p,n), \quad (11)$$

and ν_F ($F=p,n$) is related to the usual chemical potential μ_F ($F=p,n$), respectively, by

$$\nu_n = \mu_n - \frac{g_\omega^2 \rho}{m_\omega^2} + \frac{g_\rho^2}{m_\rho^2} (\rho_p - \rho_n),$$

$$\nu_p = \mu_p - \frac{g_\omega^2 \rho}{m_\omega^2} - \frac{g_\rho^2}{m_\rho^2} (\rho_p - \rho_n). \quad (12)$$

B. ρ -meson mass in a hot and dense medium

Since the details of the procedures to calculate the $NN\rho$ self-energy Feynman diagrams (Fig. 1) by TFD [29] can be found in our previous paper [26], we will only present the essential steps here which are necessary for our calculations. According to TFD, each field has double components and they lead to the 2×2 matrix propagator, but only the 1-1 component has a contribution to the self-energy. The 1-1 component of the nucleon and ρ -meson are, respectively [26,30],

$$\Delta^{11}(k) = (k \cdot \gamma + M^*) \left\{ \frac{1}{k^2 - M^{*2} + i\epsilon} + 2\pi i n_F(k) \delta(k^2 - M^{*2}) \right\}, \quad (13)$$

$$D_\rho^{\mu\nu}(k) = \left(-g^{\mu\nu} + \frac{k^\mu k^\nu}{m_\rho^2} \right) \times \left\{ \frac{1}{k^2 - m_\rho^2 + i\epsilon} - 2\pi i n_B(k) \delta(k^2 - m_\rho^2) \right\}, \quad (14)$$

where

$$N_F(k) = [\theta(k_0) n_F(k) + \theta(-k_0) \bar{n}_F(k)],$$

$$n_B(k) = \frac{1}{e^{\beta|k_0|} - 1}. \quad (15)$$

$\theta(k_0)$ is the step function and n_B the boson distribution function. It is worth noting that instead of the value M of nuclear mass in vacuum, the effective nucleon mass M^* in a hot medium occurs in the propagator Δ^{11} of the nucleon. This is obvious because on rescaling the wave function of nucleon field $\psi \rightarrow f^{1/2} \psi$ for the ZM model, the derivative coupling term between the nucleon field and σ field disappears and the Lagrangian becomes L_{ZM} [1]. The Lagrangian L_{ZM} or L_{IZM} include the effective mass M^* only, which is a function of the mean field σ . As was pointed out by many authors [26–28], the ρ -meson mass calculated by the vacuum polarization diagrams of the $NN\rho$ vector and tensor coupling interactions increases with the temperature and density. This result is obviously in conflict with recent experiments. To reconcile the discrepancy, as was pointed out by Shiomi and Hatsuda [27], the vacuum fluctuation (VF) effect must be taken into account, i.e., by changing the mass of nucleon M in vacuum in the Feynman propagator by its effective mass M^* in a hot medium and recalculation of the vacuum polarization diagrams. After this step, one can find that the ρ -meson mass in a hot medium decreases with temperature and density. In Refs. [27,28] and [26], the effective mass of nucleon is adopted from the results of MFA in the Walecka model and Bonn potential model, respectively. In our improved ZM model, the effective mass M^* occurs naturally in the Feynman propagator Δ^{11} and the VF effect has been considered in the same model self-consistently, which are the advantages of the model.

Now we turn to calculate the ρ -meson mass. The self-energy of the ρ meson under the one-loop approximation reads (Fig. 1)

$$\Pi_\rho^{\mu\nu} = -i \int \frac{d^4 k}{(2\pi)^4} \text{Tr}[\Gamma^\mu \Delta^{11}(k) \tilde{\Gamma}^\nu \Delta^{11}(k+q)], \quad (16)$$

where

$$\Gamma^\mu = \left[g_\rho \gamma^\mu - \frac{f_\rho}{2M^*} i \sigma^{\mu\lambda} q_\lambda \right] \tau_i,$$

$$\tilde{\Gamma}^\nu = \left[g_\rho \gamma^\nu + \frac{f_\rho}{2M^*} i \sigma^{\nu\lambda} q_\lambda \right] \tau_j. \quad (17)$$

A straightforward calculation can show

$$\Pi_\rho^{\mu\nu} = \Pi_{\rho F}^{\mu\nu} + \Pi_{\rho D}^{\mu\nu},$$

$$\Pi_{\rho F}^{\mu\nu} = i \int \frac{d^4 k}{(2\pi)^4} T^{\mu\nu} \frac{1}{(k^2 - M^{*2})[(k+q)^2 - M^{*2}]},$$

$$\Pi_{\rho D}^{\mu\nu} = - \int \frac{d^4k}{(2\pi)^3} T^{\mu\nu} \left\{ \frac{\delta(k^2 - M^{*2})}{(k+q)^2 - M^{*2}} N_F(k) + \frac{\delta[(k+q)^2 - M^{*2}]}{k^2 - M^{*2}} N_F(k+q) \right\}, \quad (18)$$

where

$$\begin{aligned} T^{\mu\nu} &= \text{Tr} \left[\left[g_\rho \gamma^\mu + \frac{f_\rho}{2M^*} i \sigma^{\mu\lambda} q_\lambda \right] (k \cdot \gamma + M^*) \left[g_\rho \gamma^\nu - \frac{f_\rho}{2M^*} i \sigma^{\nu\delta} q_\delta \right] (k \cdot \gamma + q \cdot \gamma + M^*) \right] \\ &= 4g_\rho^2 \{ k^\mu (k+q)^\nu + k^\nu (k+q)^\mu - g^{\mu\nu} [k \cdot (k+q) - M^{*2}] \} - 4g_\rho f_\rho (q^\mu q^\nu - q^2 g^{\mu\nu}) \\ &\quad - \frac{f_\rho^2}{M^{*2}} \{ q^\mu q^\nu (k^2 - k \cdot q + M^{*2}) - 2k \cdot q (k^\mu q^\nu + q^\mu k^\nu) + 2q^2 k^\mu k^\nu + g^{\mu\nu} [2(k \cdot q)^2 - q^2 (k^2 - k \cdot q + M^{*2})] \}. \end{aligned} \quad (19)$$

Because of the self-energy correction, the propagator of the ρ meson in the hot and dense medium reads

$$D_\rho^{\mu\nu} = - \frac{P_L^{\mu\nu}}{q^2 - m_\rho^2 - \Pi_{\rho L}} - \frac{P_T^{\mu\nu}}{q^2 - m_\rho^2 - \Pi_{\rho T}}, \quad (20)$$

where $\Pi_{\rho L}$ and $\Pi_{\rho T}$ are, respectively, the longitudinal and transverse components of the ρ -meson self-energy:

$$\Pi_{\rho L} = - \frac{q^2}{\vec{q}^2} u_\mu u_\nu \Pi_\rho^{\mu\nu}, \quad \Pi_{\rho T} = \frac{1}{2} \left(\frac{q^2}{\vec{q}^2} u_\mu u_\nu - g_{\mu\nu} \right) \Pi_\rho^{\mu\nu}. \quad (21)$$

u_μ is the four vector of the medium and in the medium rest frame, $u_\mu = (1, \vec{0})$; $P_L^{\mu\nu}$ and $P_T^{\mu\nu}$ are the projection tensors defined as

$$\begin{aligned} P_T^{00} = P_T^{0i} = P_T^{i0} = 0, \quad P_T^{ij} = \delta^{ij} - q^i q^j / q^2, \\ P_T^{\mu\nu} + P_L^{\mu\nu} = -g^{\mu\nu} + q^\mu q^\nu / q^2. \end{aligned} \quad (22)$$

The effective mass of the ρ -meson is defined as the pole of the propagator $D_\rho^{\mu\nu}$ in the limit $\vec{q} \rightarrow 0$ [26,28,31]. One can prove that, in the limit $\vec{q} \rightarrow 0$,

$$\Pi_{\rho L}(q_0, \vec{q} \rightarrow 0) = \Pi_{\rho T}(q_0, \vec{q} \rightarrow 0) = \frac{1}{3} \Pi_{\rho\mu}^\mu(q_0, \vec{q} \rightarrow 0). \quad (23)$$

The effective mass of the ρ -meson m_ρ^* then satisfies

$$m_\rho^{*2} = m_\rho^2 + \Pi_{\rho L}(q_0 = m_\rho^*, \vec{q} \rightarrow 0). \quad (24)$$

From Eqs. (18), (19), (21), and (23), we obtain

$$\begin{aligned} \Pi_{\rho L}(q_0, \vec{q} \rightarrow 0) &= \frac{g_\rho^2 q_0^2}{\pi^2} I_2 + \frac{g_\rho f_\rho}{2\pi^2} I_1 \\ &\quad + \frac{f_\rho^2 q_0^2}{8\pi^2 M^{*2}} (M^{*2} I_1 + q_0^2 I_2) \\ &\quad + \frac{4g_\rho^2}{3\pi^2} (6M^{*2} I_3 + 4I_4) + \frac{4g_\rho f_\rho}{\pi^2} q_0^2 I_3 \\ &\quad + \frac{2f_\rho^2}{3\pi^2 M^{*2}} (3q_0^2 M^{*2} I_3 - q_0^2 I_4), \end{aligned} \quad (25)$$

where I_1 , I_2 , I_3 , and I_4 are integrals as follows:

$$I_1 = \int_0^1 dx \ln \frac{M^{*2} - q_0^2 x + q_0^2 x^2}{M^2 - q_0^2 x + q_0^2 x^2},$$

$$I_2 = \int_0^1 dx x(1-x) \ln \frac{M^{*2} - q_0^2 x + q_0^2 x^2}{M^2 - q_0^2 x + q_0^2 x^2},$$

$$I_3 = \int_0^\infty dx \frac{x^2}{\varepsilon_N(x) [4\varepsilon_N^2(x) - q_0^2]} [n_F(x) + \bar{n}_F(x)],$$

$$I_4 = \int_0^\infty dx \frac{x^4}{\varepsilon_N(x) [4\varepsilon_N^2(x) - q_0^2]} [n_F(x) + \bar{n}_F(x)], \quad (26)$$

and $\varepsilon_N(x) = \sqrt{x^2 + M^{*2}}$. The effective mass m_ρ^* can be obtained from Eqs. (24) to (26) numerically.

However, there is another way to define the ρ -meson mass in a hot dense medium, i.e., the so called screening mass which is defined as the inverse Debye screening length [28,26,30,31]. The equations for defining the longitudinal screening mass $m_{\rho L}^s$ and the transverse screening mass $m_{\rho T}^s$ of the ρ meson are

$$\begin{aligned} m_{\rho L}^s &= [m_\rho^2 + \Pi_{\rho L}(0, \vec{q} \rightarrow 0)]^{1/2}, \\ m_{\rho T}^s &= [m_\rho^2 + \Pi_{\rho T}(0, \vec{q} \rightarrow 0)]^{1/2}. \end{aligned} \quad (27)$$

We can prove that

$$\begin{aligned} \Pi_{\rho L}(0, \vec{q}) &= \Pi_{\rho 00}(0, \vec{q}), \\ \Pi_{\rho T}(0, \vec{q}) &= \frac{1}{2} [\Pi_{\rho\mu}^\mu(0, \vec{q}) - \Pi_{\rho 00}(0, \vec{q})], \end{aligned} \quad (28)$$

and

$$\begin{aligned} m_{\rho L}^s &= \left[H_L \left(m_\rho^2 + \frac{4g_\rho^2}{\pi^2} I_5 \right) \right]^{1/2}, \\ m_{\rho T}^s &= \left[H_T \left(m_\rho^2 + \frac{g_\rho^2 M^{*2}}{\pi^2} I_6 \right) \right]^{1/2}, \end{aligned} \quad (29)$$

where

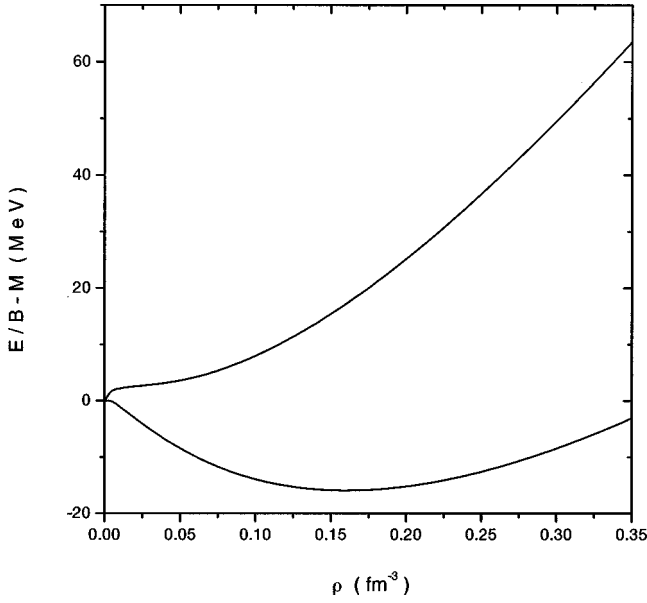


FIG. 2. The density dependence of the binding energy per nucleon. The lower curve corresponds to the symmetric nuclear matter and the upper curves to neutral nuclear matter.

$$\begin{aligned}
 H_L &= \left[1 - \frac{g_\rho(g_\rho + 2f_\rho)}{2\pi^2} I_6 + \frac{f_\rho^2}{2\pi^2} \frac{I_7}{M^{*2}} \right. \\
 &\quad \left. - \left(\frac{g_\rho^2}{3\pi^2} + \frac{g_\rho f_\rho}{\pi^2} + \frac{f_\rho^2}{4\pi^2} \right) \ln \frac{M^*}{M} \right]^{-1}, \\
 H_T &= \left[1 - \frac{g_\rho(g_\rho + 4f_\rho)}{4\pi^2} I_6 - \frac{f_\rho^2}{4\pi^2} \left(2I_6 \frac{M^2}{M^{*2}} + \frac{I_5 + I_7}{M^{*2}} \right) \right. \\
 &\quad \left. - \left(\frac{g_\rho^2}{3\pi^2} + \frac{g_\rho f_\rho}{\pi^2} + \frac{f_\rho^2}{4\pi^2} \right) \ln \frac{M^*}{M} \right]^{-1}, \quad (30)
 \end{aligned}$$

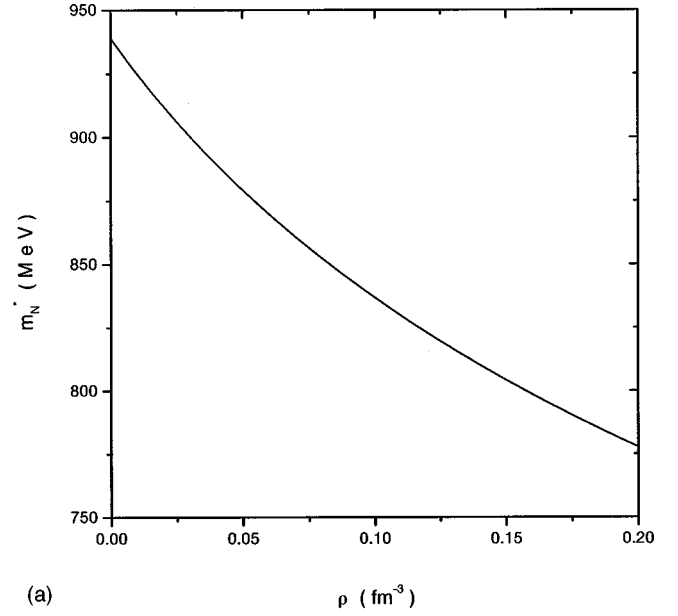
and I_5 , I_6 , and I_7 are integrals as follows:

$$\begin{aligned}
 I_5 &= \int_0^\infty dx \frac{x^2}{\varepsilon_N(x)} [n_F(x) + \bar{n}_F(x)], \\
 I_6 &= \int_0^\infty dx \frac{x^2}{\varepsilon_N^3(x)} [n_F(x) + \bar{n}_F(x)], \\
 I_7 &= \int_0^\infty dx \frac{x^4}{\varepsilon_N^3(x)} [n_F(x) + \bar{n}_F(x)]. \quad (31)
 \end{aligned}$$

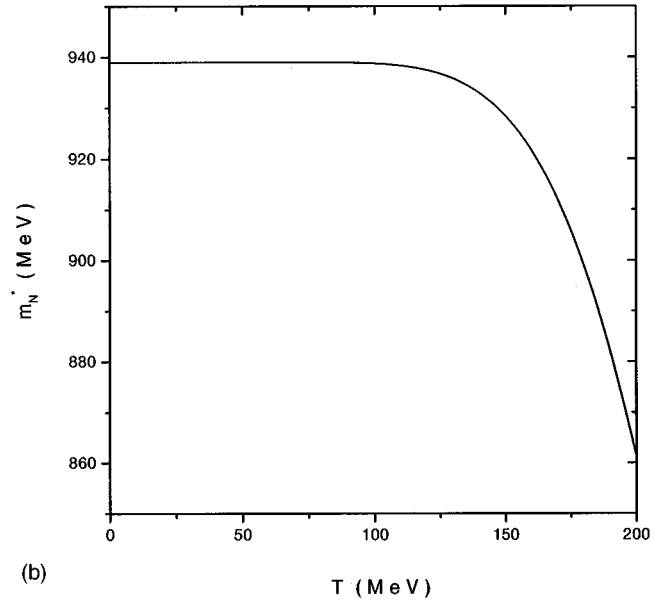
III. RESULTS AND DISCUSSIONS

Prior to the numerical calculations, we must first determine the parameters for L_{IZM} . The parameters except the vector coupling constant g_ρ and the tensor coupling constant f_ρ are chosen as those in Refs. [1,11,13] to reproduce the equilibrium properties of nuclear matter [1] and the spin-orbit splitting of nuclei [11,13]:

$$M = 939 \text{ MeV}, \quad m_\omega = 783 \text{ MeV},$$



(a)



(b)

FIG. 3. (a) The effective mass of nucleon M^* against density at zero temperature. (b) The effective mass of nucleon M^* against temperature at zero density.

$$m_\rho = 768 \text{ MeV}, \quad m_\sigma = 550 \text{ MeV},$$

$$C_\sigma^2 = \left(\frac{M^2}{m_\sigma^2} \right) g_\sigma^2 = 169.2, \quad C_\omega^2 = \left(\frac{M^2}{m_\omega^2} \right) g_\omega^2 = 59.1, \quad f_\omega = 7.0. \quad (32)$$

The vector coupling constant g_ρ is chosen to fit the symmetry energy of the nuclear matter because the tensor coupling term of $NN\rho$ interaction has no contribution to the binding energy in MFA. The curves of binding energy per nucleon against the density at zero temperature are shown in Fig. 2, where we have chosen the parameter $g_\rho = 4.23$. In this figure, the lower curve corresponds to the symmetric nuclear matter ($\rho_p = \rho_n$) and the upper curve corresponds to the neutral nuclear matter ($\rho_p = 0$). By using this figure, we find the

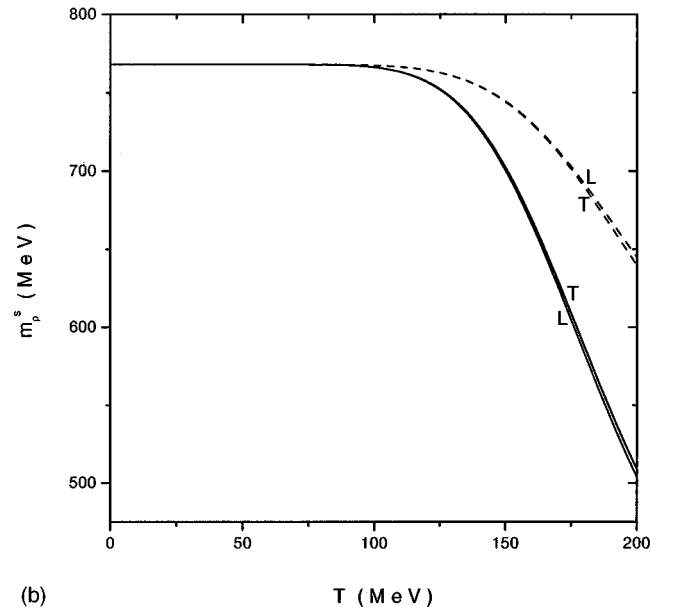
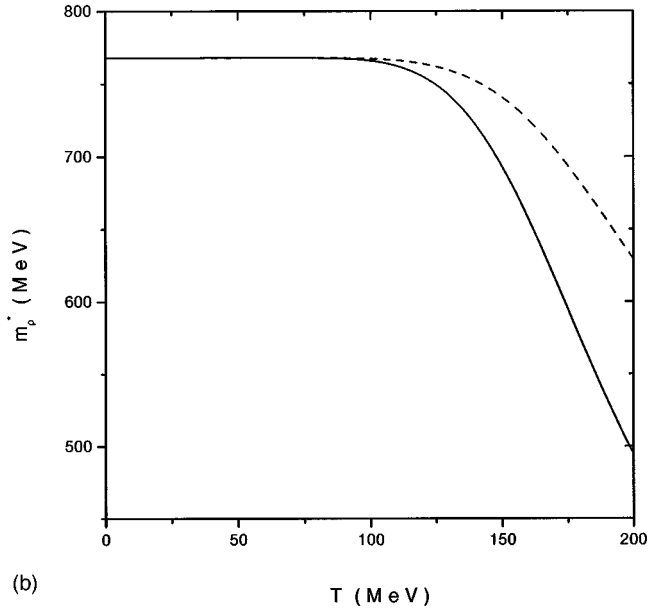
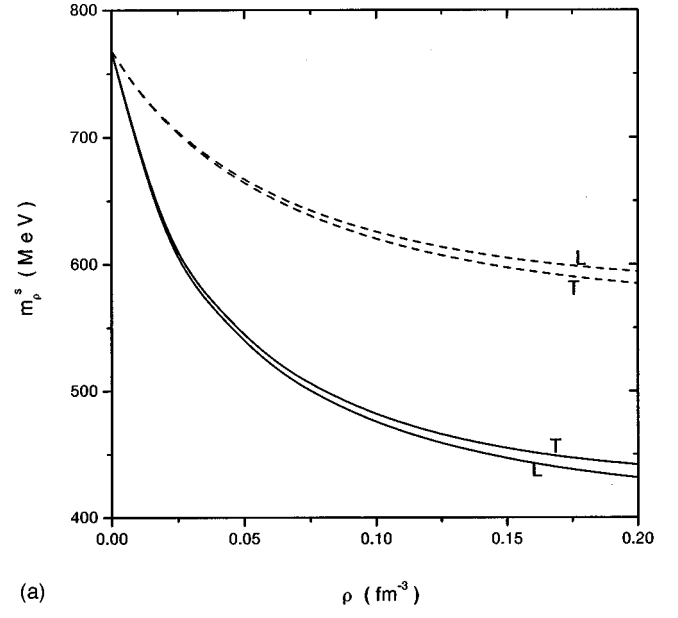
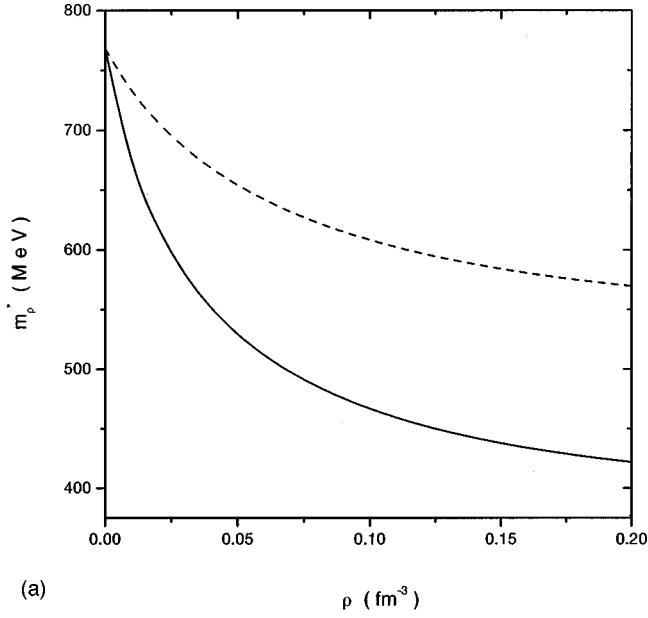


FIG. 4. (a) The density dependence of the effective mass of ρ meson at zero temperature: the solid curve corresponds to strong coupling and the dashed curve to weak coupling. (b) Same as (a), but for temperature dependence at zero density.

FIG. 5. (a) Same as Fig. 4(a), but for longitudinal screening mass (denoted by L) and for transverse screening mass (denoted by T) of ρ meson. (b) Same as (a), but for temperature dependence at zero density.

symmetry energy is 33.2 MeV, i.e., if we take $g_\rho=4.23$, we can reproduce the symmetry energy satisfactorily.

The tensor coupling constant f_ρ is chosen by strong or weak coupling. To compare with the usual $NN\rho$ vector and tensor coupling model, we define $f_\rho = \tilde{f}_\rho [1 + g_\sigma \sigma / M]^{-1}$, so the $NN\rho$ tensor coupling term of L_{IZM} becomes $(\tilde{f}_\rho / 4M) \bar{\psi} \sigma^{\mu\nu} \vec{\tau} \cdot (\partial_\mu \vec{b}_\nu - \partial_\nu \vec{b}_\mu) \psi$, which has the same form as that of $NN\rho$ vector and tensor coupling model. According to the arguments of Brown and Machleidt [32], it is better to consider the overall strength of the ρ coupling in this case, as it emerges from the calculation of a one- ρ -exchange Feynman diagram between two nucleons. The values of the overall strength are [32]

$$(g_\rho + \tilde{f}_\rho)^2 / 4\pi = \left\{ \begin{array}{l} 37 \pm 15 \text{ for H\"ohler-Pietarinen model} \\ 42.3 \text{ for Bonn potential} \\ 45.4 \text{ for Bonn } B \text{ potential} \\ 41.0 \text{ for Nijmegen potential} \end{array} \right\}$$

for strong coupling and

$$(g_\rho + \tilde{f}_\rho)^2 / 4\pi = 13.25$$

for weak coupling. In our calculations, we choose $g_\rho=4.23$ and $(g_\rho + \tilde{f}_\rho)^2 / 4\pi = 45.4$ or 13.3 for strong coupling and weak coupling to determine \tilde{f}_ρ .

Another point we hope to note before calculating the ρ -meson mass is about the effective mass of nucleon M^* . As

TABLE I. The mass of ρ meson at density of 0.12 fm^{-3} and at zero temperature where exp, WC, and SC denote values of experiment, weak coupling calculation, and strong coupling calculation, respectively.

	Density (fm^{-3})	m_{ρ}^* (MeV)	$m_{\rho L}^s$ (MeV)	$m_{\rho T}^s$ (MeV)
exp			610	
WC	0.12	597	616	609
SC		453	462	469

can be observed from Eqs. (2) and (6), M^* is determined by the exchange of σ meson only in the usual ZM model. However, in our improved ZM model, in a rigorous sense, M^* must be determined not only by the exchange of the σ meson, but also the ω meson and the ρ meson because we have $NN\omega$ and $NN\rho$ interactions in L_{IZM} . Even though the contribution of the tadpole diagram with the vector mesons exchange to the nucleon self-energy is zero, the exchange diagrams of the Hartree-Fock approximation can affect M^* . This effect had been calculated in details in our previous papers [11,26]. However, our results indicate that the effects of vector mesons exchange are very small. Even in the strong coupling approach, the reduction of M^* at the saturation density due to the exchange of vector mesons is $M^* = 0.98M$. We can neglect the contributions of the exchange of vector mesons to M^* . In fact, the main contributions of the reduction of M^* come from the exchange of scalar σ mesons. The dependent curves of M^* to density (at zero temperature) and to temperature (at zero density) are shown in Figs. 3(a) and 3(b), respectively.

Now we are in a position to address our main results, i.e., the effective mass and the screening mass of ρ meson at finite temperature and/or finite density. Our results are shown in Figs. 4(a) and 4(b) and Figs. 5(a) and 5(b). In Figs. 4(a) [and 4(b)], we show the curves of the effective mass of ρ meson m_{ρ}^* against density (temperature) at zero temperature (density), where the solid line refers to strong coupling and the dashed line to weak coupling, respectively. In Fig. 5(a) [and 5(b)], we show the curves of the screening mass of ρ

meson against density (temperature) at zero temperature (density), where L denotes the longitudinal part and T the transverse part, the solid lines refer to strong coupling and dashed lines to weak coupling. We see from these figures that all m_{ρ}^* , $m_{\rho L}^s$, and $m_{\rho T}^s$ decrease as the density (or temperature) increases for both strong coupling and weak coupling. This is reasonable because we have taken into account the vacuum fluctuation of the effective nucleon mass which make the mass of ρ meson decrease with density or temperature [26–28]. Furthermore, we see from these figures that the reductions of the ρ -meson mass for the strong coupling are faster than those for the weak coupling, which means that the tensor coupling term of $NN\rho$ plays an essential role in the reduction of the ρ -meson mass because the values of the coupling f_{ρ} are different for strong and weak couplings.

To compare our results with experiments, we list the theoretical values of ρ meson mass at the density $\rho = 0.7\rho_0 = 0.12 \text{ fm}^{-3}$ and the experimental value from the TAGX Collaboration [22] in Table I. From Table I, we see that the weak coupling results fit the experimental data very well.

In summary, to overcome the shortcomings of the ZM model, we have added the ρ -meson freedom and the tensor coupling terms to the ZM model and suggested an improved ZM Lagrangian. The freedoms in L_{IZM} are nucleons, σ mesons, ω mesons, and ρ mesons. Besides $NN\sigma$ interaction, we have $NN\rho$ and $NN\omega$ vector and tensor coupling interactions in our improved ZM Lagrangian. By using the TFD, in one-loop approximation, we have calculated the ρ -meson mass of this model at finite density and/or finite temperature. We have found that the ρ -meson mass at $\rho = 0.7\rho_0$ given by weak coupling is in good agreement with the recent TAGX experimental results. Then we come to a conclusion that the improved ZM model is successful. It can explain more experimental properties of nuclear systems than the ZM model can.

ACKNOWLEDGMENT

The present work was supported in part by the NNSF of China.

-
- [1] J. Zimany and J. A. Moszkowski, Phys. Rev. C **42**, 1416 (1990).
[2] M. Malheiro, A. Delfino, and C. T. Coelho, Phys. Rev. C **58**, 426 (1998).
[3] A. Bhattachargga and Raha, Phys. Rev. C **53**, 522 (1996).
[4] R. Aguirre, O. Eivutarese, and A. L. de Paoli, Nucl. Phys. **A597**, 543 (1996).
[5] K. Miyazaki, Prog. Theor. Phys. **93**, 137 (1995).
[6] B. D. Serot and J. D. Walecka, *Advances in Nuclear Physics*, edited by J. W. Negele and E. Vogt (Plenum, New York, 1986), Vol. 16, p. 1; Int. J. Mod. Phys. E **6**, 515 (1997).
[7] Z. X. Qian, H. Q. Song, and R. K. Su, Phys. Rev. C **48**, 154 (1993).
[8] R. K. Su, T. Long, Y. J. Zhang, P. K. N. Yu, and E. C. M. Young, Phys. Rev. C **55**, 2373 (1995).
[9] H. Q. Song, Z. X. Qian, and R. K. Su, Phys. Rev. C **49**, 2924 (1994).
[10] R. K. Su, S. D. Yang, and T. T. S. Kuo, Phys. Rev. C **35**, 1539 (1994); R. K. Su, T. Long, and Y. J. Zhang, *ibid.* **51**, 1265 (1995); H. Q. Song, Z. X. Qian, and R. K. Su, *ibid.* **47**, 2001 (1993).
[11] R. K. Su, L. Li, and H. Q. Song, J. Phys. G **24**, 1735 (1998).
[12] A. Delfino, M. Chiapparini, M. Malheiro, L. V. Belvedere, and A. O. Gattone, Z. Phys. A **355**, 145 (1996).
[13] T. S. Biro and J. Zimanyi, Phys. Lett. B **391**, 1 (1997).
[14] M. Masera *et al.*, Nucl. Phys. **A590**, 93c (1996); Th. Ullrich *et al.*, *ibid.* **A610**, 317c (1996); E. Scomparin *et al.*, *ibid.* **A610**, 331c (1996).
[15] G. Q. Li, C. M. Ko, and G. E. Brown, Phys. Rev. Lett. **75**, 4007 (1995).
[16] L. A. Kondratyuk, A. Sibirtsev, W. Cassing, Ye. S. Golubeva, and M. Effenberger, Phys. Rev. C **58**, 1078 (1998).
[17] V. L. Eletsky and B. L. Ioffe, Phys. Rev. Lett. **78**, 1010 (1997).

- [18] F. Klingl and W. Weise, Nucl. Phys. **A606**, 329 (1996).
- [19] T. Waas, H. Rho, and W. Weise, Nucl. Phys. **A617**, 449 (1997).
- [20] R. Rapp, G. Chanfray, and J. Wambach, Nucl. Phys. **A617**, 472 (1997).
- [21] S. Gao, Y. J. Zhang, and R. K. Su, J. Phys. G **21**, 1665 (1995).
- [22] G. J. Lolos *et al.*, Phys. Rev. Lett. **80**, 241 (1998).
- [23] G. E. Brown and M. Rho, Phys. Rev. Lett. **66**, 2720 (1991).
- [24] T. Hatsuda and Su. H. Lee, Phys. Rev. C **46**, R34 (1993); M. Asakawa and C. M. Ko, *ibid.* **48**, R526 (1993); T. Hatsuda, Y. Koiko, and Su. H. Lee, Nucl. Phys. **B394**, 221 (1993).
- [25] K. Saito, K. Tsushima, and A. W. Thomas, Phys. Rev. C **56**, 566 (1997).
- [26] Y. J. Zhang, S. Gao, and R. K. Su, Phys. Rev. C **56**, 3336 (1997).
- [27] H. Shiomi and T. Hatsuda, Phys. Lett. B **334**, 281 (1994).
- [28] C. Song, P. W. Xia, and C. M. Ko, Phys. Rev. C **52**, 408 (1995).
- [29] H. Umezawa, H. Matsumoto, and M. Tachiki, *Thermo Field Dynamics and Condensed States* (North-Holland, Amsterdam, 1982).
- [30] S. Gao, R. K. Su, and P. K. N. Yu, Phys. Rev. C **49**, 40 (1994); S. Gao, Y. J. Zhang, and R. K. Su, Nucl. Phys. **A593**, 362 (1995).
- [31] S. Gao, Y. J. Zhang, and R. K. Su, Phys. Rev. C **52**, 380 (1995).
- [32] G. E. Brown and R. Machleidt, Phys. Rev. C **50**, 1731 (1994).